Neuron, Vol. 19, 1237–1248, December, 1997, Copyright ©1997 by Cell Press

Genetic Analysis of Glutamate Receptors in Drosophila Reveals a Retrograde Signal Regulating Presynaptic Transmitter Release

Sophie A. Petersen, Richard D. Fetter, Jasprina N. Noordermeer, Corey S. Goodman,* and Aaron DiAntonio
Howard Hughes Medical Institute
Department of Molecular and Cell Biology
University of California
Berkeley, California 94720

Summary

Postsynaptic sensitivity to glutamate was genetically manipulated at the Drosophila neuromuscular junction (NMJ) to test whether postsynaptic activity can regulate presynaptic function during development. We cloned the gene encoding a second muscle-specific glutamate receptor, DGluRIIB, which is closely related to the previously identified DGluRIIA and located adjacent to it in the genome. Mutations that eliminate *DGluRIIA* (but not *DGluRIIB*) or transgenic constructs that increase *DGluRIIA* expression were generated. When *DGluRIIA* is missing, the response of the muscle to a single vesicle of transmitter is substantially decreased. However, the response of the muscle to nerve stimulation is normal because quantal content is significantly increased. Thus, a decrease in postsynaptic receptors leads to an increase in presynaptic transmitter release, indicating that postsynaptic activity controls a retrograde signal that regulates presynaptic function.

Introduction

Activity-dependent mechanisms play a central role in shaping the pattern and strength of synaptic connections as they form during development and are modified during learning and memory throughout life (e.g., Goodman and Shatz, 1993; Bailey et al., 1996). Evidence has begun to accumulate that suggests a role of postsynaptic activity in the regulation of presynaptic structure and function during development in systems ranging from the neuromuscular junction (NMJ; Dan and Poo, 1994; Nguyen and Lichtman, 1996) to the retinotectal projection (Cline, 1991). In the adult, long-term potentiation (LTP) in the hippocampus also appears to make use of a retrograde mechanism for strengthening synaptic connections (Larkman and Jack, 1995).

Our goal in the present study was to establish a genetic model that could be used to dissect the molecular mechanisms of retrograde signaling that control synaptic strength during development. We presume that such a mechanism might be used more generally in the regulation of synaptic plasticity. We chose the Drosophila neuromuscular junction (NMJ) for these studies because it is possible to manipulate the genotype of the pre- or postsynaptic cell independently and to study the consequences on both the structure and the function of the synapse in vivo.

The Drosophila NMJ shares several important features with central excitatory synapses in the vertebrate brain: it is glutamatergic, with homologous ionotropic glutamate receptors, and it is organized into a series of boutons that can be added or eliminated during development and plasticity. In addition, both the Drosophila NMJ and vertebrate central synapses exhibit dynamic functional plasticity. In Drosophila, this plasticity is revealed by genetic manipulations that alter neuronal excitability (*eag Sh*; Budnik et al., 1990), second messengers (*dnc*; Zhong and Wu, 1991), protein kinases (*CamKII*; Wang et al., 1994), linker proteins (*dlg*; Budnik et al., 1996), cell adhesion molecules (*FasII*; Schuster et al., 1996a, 1996b; Stewart et al., 1996; *FasI*; Zhong and Shanley, 1995), and transcription factors (CREB; Davis et al., 1996). All of these previous genetic manipulations have altered both the pre- and postsynaptic cells, so it has not been possible to assess the role of the target cell in synaptic plasticity. In the present study, we target the postsynaptic cell in our genetic manipulation of synaptic function.

The developmental history of the Drosophila NMJ makes it a good candidate synapse for retrograde regulation. As the Drosophila larvae develops from the first to third instar over a period of several days, there is at least a 100-fold increase in the surface area of the postsynaptic muscle. This increase in size leads to a dramatic decrease in input resistance, so that a larger synaptic current is required to depolarize the muscle. During this developmental period, there is a concomitant growth of the presynaptic nerve terminal, resulting in an increased number of both boutons and active zones per bouton. In fact, there is a tight correlation between muscle size and the number of synaptic boutons (Schuster et al., 1996a). We have investigated whether these two synchronous developmental events are autonomous or, alternatively, whether there is an activity-dependent signaling mechanism that ensures appropriate innervation. We tested the hypothesis that synaptic growth and plasticity are regulated by activity in the muscle by genetically manipulating postsynaptic sensitivity to glutamate.

A gene encoding one muscle-specific glutamate receptor, DGluRII, was identified previously in Drosophila (Schuster et al., 1991). This ionotropic receptor is a non-NMDA type but can not be classified as an AMPA or kainate type by sequence. It is expressed in all somatic muscles and is excluded from the nervous system (Currie et al., 1995). This receptor localizes to synaptic boutons during late embryogenesis (Saitoe et al., 1997). We have now identified a gene encoding a second muscle-specific glutamate receptor, DGluRIIB. We show that DGluRII (here renamed DGluRIIA) and DGluRIIB localize to hot spots within synaptic boutons at the mature third instar NMJ.

We have generated loss-of-function mutants of *DGluRIIA* that have a decreased sensitivity to transmitter

*To whom correspondence should be addressed.

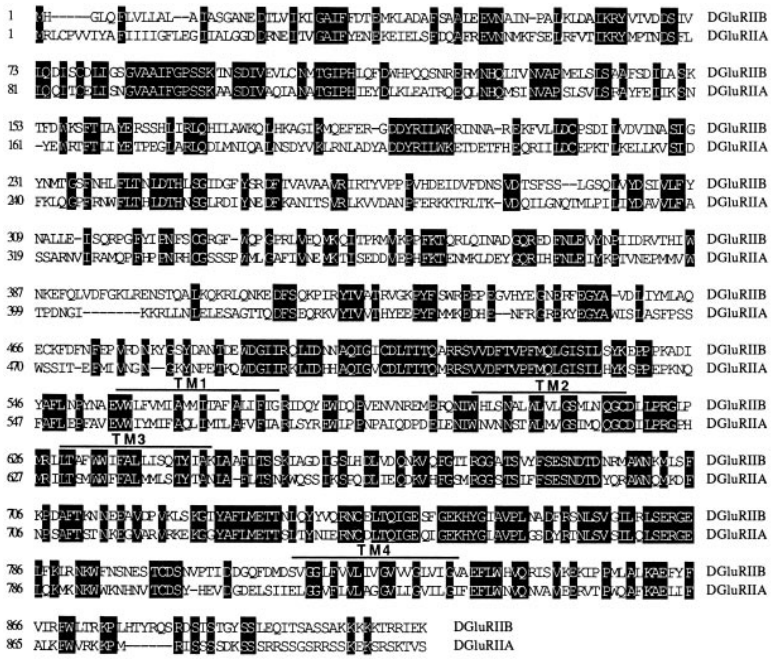

Figure 1. Sequence of *DGluRIIB*

The predicted amino acid sequences of *DGluRIIB* and *DGluRIIA* are aligned, and identical amino acids are shaded. The putative transmembrane and pore forming domains (TM1–TM4) are noted.

and gain-of-function mutants, in which *DGluRIIA* is overexpressed, that have an increased sensitivity to transmitter. Analysis of these mutants reveals that a decreased postsynaptic sensitivity is compensated for by an increase in transmitter release from the neuron. The presynaptic neuron is thus regulated in response to a physiological change in the postsynaptic cell, indicating the existence of a retrograde signaling mechanism. This signaling mechanism may be used to ensure that the muscle receives adequate amounts of transmitter during its rapid growth from embryonic to larval stages.

Results

A Second Muscle-Specific Glutamate Receptor Is Localized to Active Zones at the NMJ

Prior to this study, three ionotropic glutamate receptors had been identified in Drosophila: *DGluRI*, a kainate-type receptor expressed in the CNS; *DGluRII*, a muscle-specific AMPA/kainate-type receptor expressed in muscle; and *DNMDAR*, an NMDA-like receptor expressed in brain (Betz et al., 1993). We have identified a novel glutamate receptor, *DGluRIIB*, that is expressed in muscle and that shares significant sequence similarity to *DGluRII*. We name this new gene *DGluRIIB* and change the name of *DGluRII* to *DGluRIIA*.

DGluRIIA and DGluRIIB share 44% amino acid identity overall, with 51% identity in the highly conserved transmembrane region (Figure 1A). Sequence analysis indicates that they are members of the AMPA/kainate supergroup but does not clearly classify them as either AMPA or kainate subtypes. The two receptors are more closely related to each other than to any other known glutamate receptor. In vertebrates, the calcium permeability of AMPA/kainate receptors is determined by the presence of a glutamine or arginine within the putative pore region (Jonas and Burnashev, 1995). The sequence around this region (MQQ) is highly conserved and is present in DGluRIIA. However, in DGluRIIB, this sequence is LNQ, suggesting that the two receptors may differ in their physiological properties. Both receptors have numerous potential phosphorylation sites in their intracellular cytoplasmic tail; however, only DGluRIIA contains the ideal consensus site (RRXS) for protein kinase A. The clustering of some synaptic proteins is mediated by interactions between their C-terminal tails and a class of proteins containing protein–protein interaction modules known as PDZ domains (Sheng, 1996). Neither DGluRIIA nor DGluRIIB contains a C-terminal sequence indicative of such an interaction.

The RNA expression pattern of *DGluRIIB* was established by means of embryonic whole-mount in situ hybridization. *DGluRIIB* RNA is observed exclusively in muscle. It first appears at late stage 12 and reaches its highest levels at stage 14 (Figure 2A). In stages 15–17, *DGluRIIB* expression is lower but is still present in somatic musculature. Low levels are observed in the gut-associated muscle (data not shown). This expression pattern is similar but not identical to that of *DGluRIIA*. *DGluRIIA* is also first observed at stage 12 and is expressed exclusively in muscle, but in contrast to *DGluRIIB* it increases gradually until it reaches its highest levels in stages 16 and 17 (data not shown; Currie et al., 1995).

To investigate the subcellular localization of DGluRIIA and DGluRIIB, we tagged each receptor with the myc-epitope. The epitope was incorporated immediately following a heterologous signal sequence that was used to replace the endogenous signal sequences of each gene. As such, the myc-epitope is present at the extracellular N terminus of each receptor. Transgenic flies were generated that express the tagged receptors under the control of the muscle-specific myosin heavy-chain promoter. Both DGluRIIB (Figures 2B, 2C, and 2E) and DGluRIIA (Figure 2D) are localized to the NMJs of body-wall muscles in third instar larvae.

The NMJs of third instar larvae have been subdivided

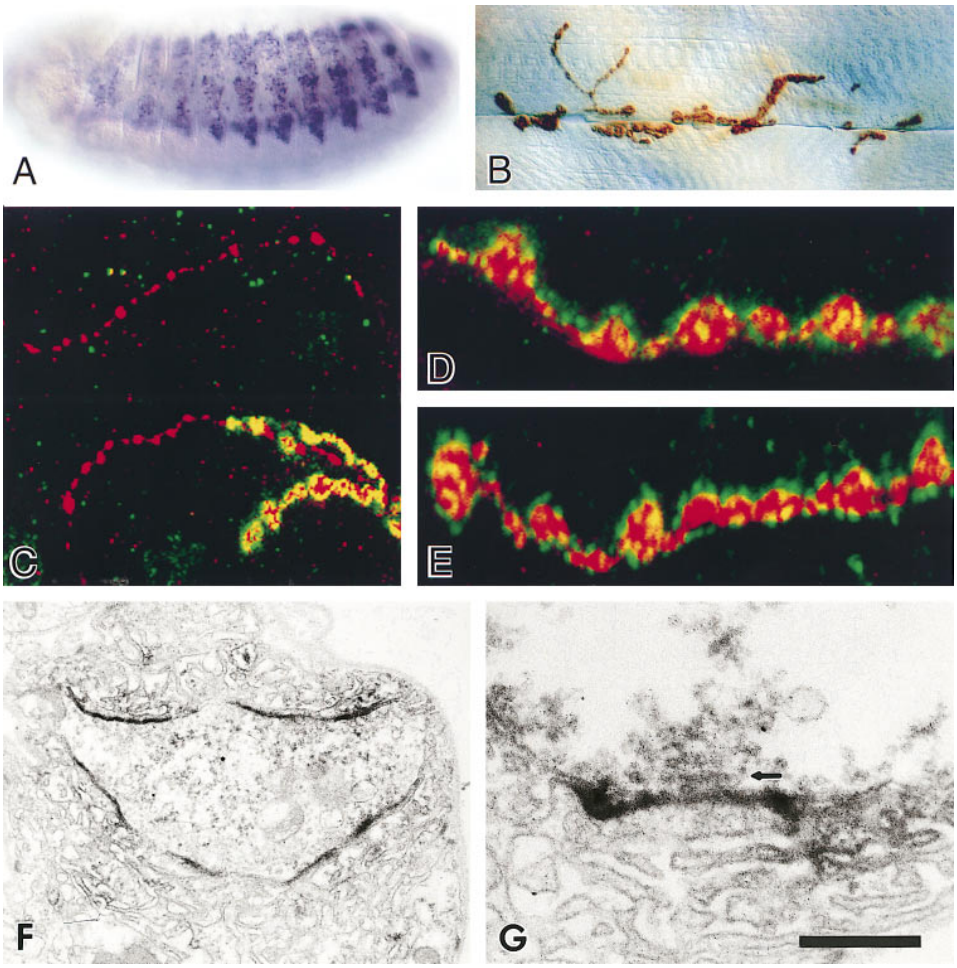

Figure 2. DGluRIIB and DGluRIIA Cluster at Boutons of Type I Synapses

(A) In situ hybridization demonstrates that *DGluRIIB* mRNA is expressed in somatic mesoderm and is not present in the nervous system. The peak of embryonic expression is seen in stage 14 embryos.

(B) HRP immunocytochemistry reveals that myc-tagged DGluRIIB is localized to the synapse at muscles 6 and 7 in third instar larvae.

(C–E) Confocal fluorescence microscopy of anti-Syt (red) and anti-myc GluR (green). In (C), myc–GluRIIB is localized to Type I synapses but not Type II synapses in third instar larvae. A high magnification view of Type I boutons reveals that (D) myc–DGluRIIA and (E) myc–DGluRIIB cluster at hot spots around the presynaptic terminal.

(F–G) Immunoelectron micrographs using the anti-myc mAb show localization of myc–GluRIIB (F) and myc–GluRIIA (G) to discontinuous patches along the synaptic cleft. A high magnification micrograph (G) demonstrates that receptors cluster opposite a presynaptic terminal containing an accumulation of synaptic vesicles and a T-bar, a T-shaped electron-dense structure typically found at presynaptic release sites in Drosophila neurons (indicated by arrow; cf. Figure 9, Atwood et al., 1993).

Scale bar, 125 μm (A); 50 μm (B); 25 μm (C); 10 μm (D and E); 1 μm (F); and 700 nm (G).

by morphological and physiological criteria. Type I synapses have larger boutons and contain small, clear, glutamate-filled vesicles, while Type II synapses have small boutons and are primarily peptidergic (Jia et al., 1993). While many muscles possess only Type I synapses, a number of muscles are innervated by both Type I and Type II synapses. To assess whether glutamate receptors are differentially localized to a particular class of synapse within a single cell, we double stained for synaptotagmin (in red), a marker of all presynaptic terminals (DiAntonio et al., 1993; Littleton et al., 1993), and for glutamate receptor (in green). Confocal microscopy reveals that DGluRIIB is localized to the postsynaptic specialization surrounding presynaptic terminals of Type I boutons, but no staining for receptors is observed at Type II boutons (Figure 2C). Staining for DGluRIIA gives the same result (data not shown). This indicates that at the Drosophila NMJ, as in vertebrate central neurons (Craig et al., 1993; Rubio and Wenthold, 1997), glutamate receptors are differentially localized to particular synapses within a single cell.

A hallmark of Type I boutons is the presence of an elaborate postsynaptic specialization, the subsynaptic reticulum (SSR), that consists of numerous layers of invaginated membrane surrounding the presynaptic terminal. Molecules localized to the SSR such as the PDZ-containing protein Discs-Large (Dlg) and the cell adhesion molecule Fasciclin II (FasII) appear to form a halo surrounding the entire presynaptic terminal when analyzed by confocal microscopy (Budnik et al., 1996; Schuster et al., 1996a). In contrast, both DGluRIIA (Figure 2D) and DGluRIIB (Figure 2E) appear as bright spots

adjacent to the presynaptic terminal. These hot spots of receptor localization are of the appropriate size and pattern to represent postsynaptic receptor clusters opposite presynaptic release sites. To investigate this possibility we performed immunoelectron microscopy. The EM analysis confirms the patchy distribution of receptors surrounding the bouton (DGluRIIB, Figure 2F; DGluRIIA, Figure 2G). Receptors are localized to particular regions of the synaptic cleft and are nearly undetectable in the underlying invaginations of the SSR. These patches of receptors around synaptic boutons are always observed opposite a presynaptic terminal containing accumulations of synaptic vesicles and tightly apposed, parallel pre- and postsynaptic membranes that are characteristic of active zones (n = 37 patches from 6 boutons). Hence, the clusters of receptors visible by confocal microscopy appear to be postsynaptic markers of vesicle release sites.

Shaker (Sh) potassium channels and FasII require Dlg for clustering at synapses (Tejedor et al., 1997; Zito et al., 1997). We wondered whether DGluRIIA or DGluRIIB also require Dlg for their localization. To address this question, we stained the myc-tagged proteins in a *dlg* mutant, dlg^{m52}, in which Sh fails to cluster to the NMJ (Tejedor et al., 1997) and found no change in glutamate receptor localization (data not shown). Hence, other proteins are likely to function in the localization of these glutamate receptors.

Genetic Deletions of *DGluRIIA* Are Viable

In order to manipulate postsynaptic sensitivity to transmitter, we began a genetic analysis of *DGluRIIA* and *DGluRIIB*. *DGluRIIB* is adjacent to *DGluRIIA* in the genome, at 25F on the left arm of chromosome 2. Sequence analysis of the genomic region encompassing both genes demonstrates that their genomic organization is quite similar (Figure 3A). With the exception of two introns in *DGluRIIB* and one in *DGluRIIA*, which do not have homologous introns in the other gene, the introns are in the same relative position in the protein sequence. A comparison of the sequence of the genomic DNA versus cDNA clones revealed no RNA editing. However, since RNA editing may occur in only a fraction of cDNAs, we cannot rule out the presence of an infrequently edited site. The sequence of putative promoter regions and introns of the two genes do not share any gross homology.

To generate mutations in *DGluRIIA*, a local P-element hopping strategy was used (Figure 3B). A P element (*P[w⁺11511]*) 15 kb upstream of *DGluRIIA* was mobilized, and insertions near *DGluRIIA* were identified by long-range PCR. An insertion 300 bp upstream of *DGluRIIA* was imprecisely excised to generate a mutation, $DGluRIIA^{SP16}$, which deletes 8 kb upstream of the insert and 1 kb into the gene itself. We believe this allele is a null mutation because the deletion removes almost the entire extracellular N-terminal domain that is likely to bind glutamate (Wo and Oswald, 1995). In addition, antibody staining with an antibody specific to the C terminus of DGluRIIA (Saitoe et al., 1997) and whole-mount RNA in situ hybridization demonstrate that no DGluRIIA mRNA or protein can be detected in this mutant (data not shown).

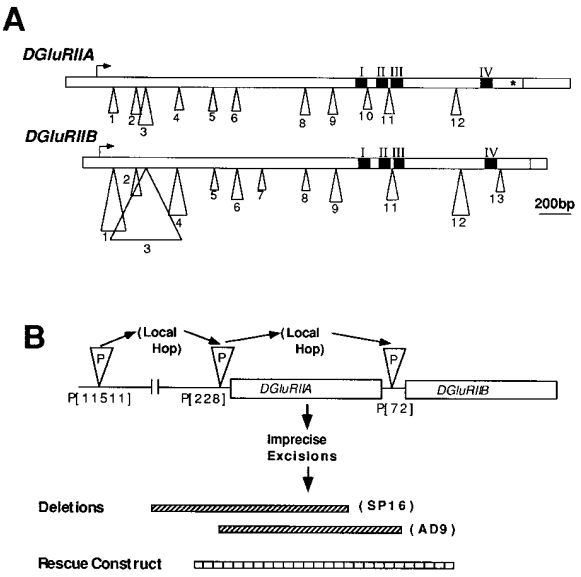

Figure 3. Genetic Analysis of *DGluRIIA* and *DGluRIIB*

(A) The exon–intron structure of *DGluRIIA* and *DGluRIIB*. Introns are numbered identically in each gene when they interrupt the cDNA sequence at homologous positions. The two genes are adjacent in the genome at chromosomal position 25F. The four putative transmembrane and pore-forming domains are indicated by black shading. The star indicates the location of the optimal PKA consensus site (RRXS).

(B) Excisions of *DGluRIIA* were generated by local hop P-element mutagenesis. A P element (P[w^+11511]) 15 kb upstream of *DGluRIIA* was mobilized, and inserts were identified near the *DGluRIIA* coding region. Successive rounds of hops and imprecise excisions were performed to generate two deletions (*SP16* and *AD9*) of *DGluRIIA*. The physiological phenotypes of *DGluRIIA* mutants were rescued by the transgenic expression of the genomic region encompassing *DGluRIIA*.

A second null allele of *DGluRIIA* was created by mobilizing *P[w^+228]* to create a line with a second insertion in the region between *DGluRIIA* and *DGluRIIB*. A null mutant ($DGluRIIA^{AD9}$) was created in which the two P elements were excised simultaneously, deleting all of the DNA between them and removing the entire coding region of *DGluRIIA*.

Both null alleles, $DGluRIIA^{SP16}$ and $DGluRIIA^{AD9}$, are completely viable and have no obvious behavioral abnormalities. These alleles do have a physiological phenotype (see below), which can be completely rescued by transgenic addition of a construct containing genomic *DGluRIIA* (Figures 3B and 4).

DGluRIIA Mutants Exhibit a Large Decrease in Quantal Size with No Change in Evoked Release, Indicating a Compensatory Increase in Quantal Content

To investigate the physiological consequences of deleting the *DGluRIIA* gene, we performed intracellular recordings from muscle 6, segment A3 of female third instar larvae. This muscle was selected because it is only innervated by the Type I boutons at which glutamate receptors cluster. In this preparation, it is possible to assess the postsynaptic response to both spontaneous

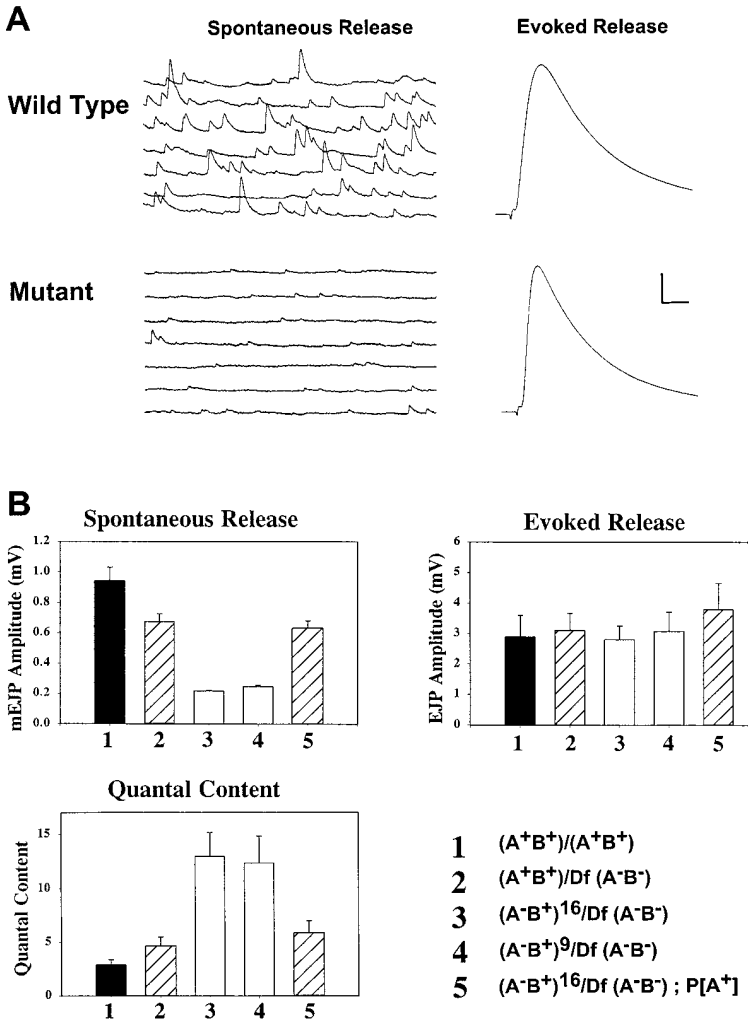

Figure 4. *DGluRIIA* Mutants Have Decreased Sensitivity to Transmitter and a Compensatory Increase in Quantal Content

(A) Representative traces of spontaneous and evoked transmitter release recorded in 0.42 mM calcium from muscle 6, segment A3 of wild-type (*Canton S*) and mutant (*DGluRIIA^{SP16}/Df(2L)cl^{h4}*) third instar larvae. Scale bar: vertical axis, 2 mV; horizontal axis, 200 ms (spontaneous release) and 16 ms (evoked release).

(B) The mean ± SEM for the mEJP amplitude, EJP amplitude, and quantal content is shown for five genotypes recorded in 0.3 mM calcium from muscle 6, segment A3 of third instar larvae: (1) wild type (*Canton S*; n = 10), (2) the parental chromosome from which the *DGluRIIA* mutants were generated in combination with a deficiency that removes both *DGluRIIA* and *DGluRIIB* (*P[w$^+$228]/Df(2L)cl^{h4}*; n = 9), (3) a deletion of *DGluRIIA* (*DGluRIIA^{SP16}/Df(2L)cl^{h4}*; n = 9), (4) a second, independent deletion of *DGluRIIA* (*DGluRIIA^{AD9}/Df(2L)cl^{h4}*; n = 9), and (5) the *DGluRIIA* mutant in (3) rescued by a *DGluRIIA* genomic transgene (*P[DGluRIIAg]/+; DGluRIIA^{SP16}/Df(2L)cl^{h4}*; n = 11). The mean quantal content was determined for each recording by dividing the average suprathreshold EJP amplitude (n = 75) by the average amplitude of the spontaneous miniature events (n > 60). In the absence of DGluRIIA, the kinetics of depolarization are altered such that the EJP is almost 40% narrower (EJP width at the half-maximal amplitude, 28.7 ± 2.5 ms (n = 7) versus 470.0 ± 3.2 ms (n = 7); p < 0.001) when comparing cells with no difference in either resting potential or mean EJP amplitude. Mean resting potential ± SEM was (1) 66.9 ± 1.1 mV, (2) 69.8 ± 1.4 mV, (3) 68.9 ± 2.2 mV, (4) 70.2 ± 1.9 mV, and (5) 69.5 ± 1.2 mV.

and evoked transmitter release. The mean amplitude of spontaneous miniature excitatory junctional potentials (mEJPs), or quantal size, is a measure of postsynaptic sensitivity to transmitter while the response to evoked excitatory junctional potentials (EJPs) depends on both the postsynaptic sensitivity and the number of transmitter-filled vesicles released from the presynaptic neuron.

To avoid complications from second-site mutations that may have been introduced on the mutagenized chromosomes, two excisions that delete *DGluRIIA* but leave *DGluRIIB* intact (*DGluRIIA^{SP16}* and *DGluRIIA^{AD9}*) were studied in combination with a genetically unrelated deficiency chromosome, *Df(2L)cl^{h4}*. This deficiency was shown by both quantitative genomic Southern analysis and in situ hybridization to delete both *DGluRIIA* and *DGluRIIB* (data not shown). A number of control lines were studied including a wild-type strain, *Canton S*, and the parental chromosome, *P[w$^+$228]*, from which the excisions were generated, in combination with *Df(2L)cl^{h4}*. Finally, the combination of the excision *DGluRIIA^{SP16}* with *Df(2L)cl^{h4}* was analyzed with the addition of a transgenic rescue construct made from the genomic region of *DGluRIIA* (*P[DGluRIIAg]*).

The most striking physiological deficit observed in the *DGluRIIA* mutants was a significant decrease in postsynaptic response to spontaneous transmitter release (Figures 4A and 4B). In the wild-type strain *Canton S*, the mean amplitude of mEJPs was 0.94 ± 0.09 mV (Figure 4B[1]). The second control line, *P[w$^+$228]/Df(2L)cl^{h4}*, which has a 50% reduction in both DGluRIIA and DGluRIIB, shows a small but significant decrease in mEJP amplitude to 0.67 ± 0.05 mV (Figure 4B[2]; p < 0.05, Student's t test). Both mutant lines, with no DGluRIIA and a 50% reduction in DGluRIIB, show a ~75% decrease in mEJP amplitude when compared to *Canton S* (Figures 4B[3] and 4B[4]; p < 0.001). This dramatic reduction in quantal size in the *DGluRIIA^{SP16}/Df(2L)cl^{h4}* mutant is rescued by a genomic *DGluRIIA* transgene (Figure 4B[5]; p < 0.001). The rescued mutant has an almost identical mean mEJP amplitude as its matched control line, *P[w$^+$228]/Df(2L)cl^{h4}* (0.63 ± 0.05 mV versus 0.67 ± 0.05 mV), indicating that the rescue transgene functions similarly to the endogenous *DGluRIIA* locus. There was no significant difference in resting membrane potential in these five genotypes. These data demonstrate that in the absence of DGluRIIA quantal size is decreased.

The measurable frequency of spontaneous mEJPs

was also decreased in the absence of DGluRIIA. There was no difference in the frequency of spontaneous events in the three control lines that express DGluRIIA (*Canton S* = 3.4 ± 0.3 Hz; *P[w⁺228]/Df(2L)cl^{h4}* = 3.4 ± 0.6 Hz; *DGluRIIA^{SP16}/Df(2L)clh4; P[DGluRIIA]* = 3.6 ± 0.5 Hz). However, the mEJP frequency in the two mutant lines was significantly decreased (*DGluRIIA^{SP16}/Df(2L)cl^{h4}* = 1.9 ± 0.2 Hz; *DGluRIIA^{AD9}/Df(2L)cl^{h4}* = 1.9 ± 0.3 Hz; $p < 0.05$). Because of the substantial decrease in quantal size in the mutant, many of the smallest spontaneous events are difficult to resolve from the noise, and no conclusion can be drawn about the presynaptic rate of spontaneous vesicle fusions.

Stimulation of the motor neuron allows for the analysis of the amplitude of the excitatory junctional potential (EJP). There was no change in the peak amplitude response to evoked transmitter release in any of the five lines that were analyzed (Figures 4A and 4B). In light of the previous finding that quantal size is decreased (see above), this result suggests that there is an increase in the number of vesicles released (quantal content) in these mutants. An estimate of quantal content can be obtained by dividing the mean EJP amplitude by the mean mEJP amplitude. This method will tend to underestimate quantal content in the mutants because the smallest mEJPs are probably lost in the noise so that the mean mEJP amplitude is overestimated. Nevertheless, this method of calculating quantal content indicates that in *DGluRIIA* mutants there is indeed a 2- to 4-fold upregulation of transmitter release ($p < 0.001$; Figure 4B). The increase in quantal content is rescued by the *DGluRIIA* transgene ($p < 0.01$). We have also used a *DGluRIIA* cDNA expressed from the muscle-specific myosin heavy-chain promoter to rescue both the decrease in quantal size ($p < 0.001$) and the increase in quantal content ($p < 0.002$) seen in the *DGluRIIA^{SP16}/Df(2L)cl^{h4}* mutant (data not shown).

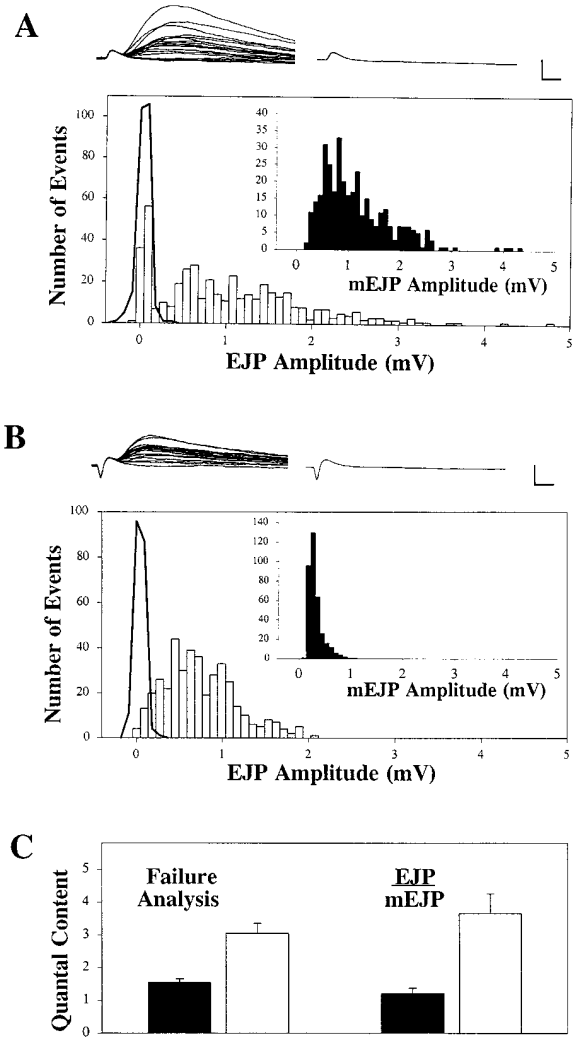

Figure 5. Failure Analysis Confirms an Increase in Quantal Content

Frequency histograms of evoked release recorded in 0.25 mM calcium from muscle 6, segment A3 of (A) wild-type (*Canton S*) and (B) mutant (*DGluRIIA^{SP16}/Df(2L)cl^{h4}*) third instar larvae. Twenty consecutive traces from each genotype are shown above the histogram and demonstrate that following the stimulus artifact release events are separated from failures. A trace average of 10 failures is shown adjacent to the consecutive traces. Amplitudes of evoked events are plotted in open bars; amplitudes of noise measurements are shown as the black line; amplitudes of spontaneous mEJPs are plotted in the inset in closed bars. Evoked events within the distribution of the noise measurement and separated from the mEJP distribution are considered failures. In (A), N = 444 and n_0 = 95 and in (B), N = 401 and n_0 = 20, where N is the number of trials and n_0 is the number of failures. The scale bar is 1 mV by 5 ms. In (C), quantal content is shown as the mean ± SEM and was estimated by the method of failures (ln [N/n_0]) and by dividing the average EJP amplitude ($n > 300$) by the average mEJP amplitude ($n > 70$) for wild type (*Canton S*; closed bars; n = 9 cells) and mutant (*DGluRIIA^{SP16}/Df(2L)cl^{h4}*; open bars; n = 10 cells). Both methods demonstrate a significant increase in quantal content in the mutant ($p < 0.001$, failure analysis; $p < 0.005$, EJP/mEJP).

Failure Analysis Confirms an Increase in Quantal Content in *DGluRIIA* Mutants

The estimate of quantal content derived from EJP/mEJP is based on the assumption that evoked and spontaneous release make use of the same pool of vesicles. A second, independent estimate of quantal content, based on failure analysis, does not require this assumption. Instead, failure analysis is based on the assumption that transmitter release will follow Poisson statistics when the probability of release approaches zero from a large number of independent release sites. At this synapse, the requirement for large numbers of release sites is satisfied since there are ~100 boutons each containing from 10–40 active zones (Atwood et al., 1993). Also, the probability of release can be decreased to near zero by lowering the external calcium concentration. Under these conditions, the Poisson model estimates quantal content as the natural log of the ratio of trials of nerve stimulation to the number of failures of the nerve to release transmitter.

We have analyzed the ratio of observed release events to the total number of trials for both wild type (*Canton S*) and the *DGluRIIA* mutant *DGluRIIA^{SP16}/Df(2L)cl^{h4}* (Figure 5). Many fewer failures were observed in the mutant than in wild type. Failure analysis indicates that quantal content is doubled in the *DGluRIIA* mutants ($p < 0.001$). The measurement of quantal content in the mutant may be an underestimate, since the very small quantal size

in the mutant will lead to the occasional misidentification of a release event as a failure. This source of error would understate the magnitude of the difference between the mutant and wild-type synapses.

The same data analyzed by the method of failures was used to estimate quantal content by EJP/mEJP. Both methods give similar estimates of quantal content (Figure 5C). This excellent agreement between independent methods of analysis suggests that this synapse obeys Poisson statistics and that here, as at the vertebrate NMJ, evoked and spontaneous release are derived from the same pool of vesicles (Jan and Jan, 1976). In addition, both methods demonstrate an increase in quantal content in the mutant. In sum, these data show that a postsynaptic defect leads to an increase in presynaptic transmitter release, demonstrating the existence of a retrograde mechanism for regulating synaptic strength.

The Up-Regulation of Transmitter Release Is Observed over a Range of Calcium Concentrations

An increase in transmitter release may be due to a physiological change in the presynaptic terminal or could result from a structural change such as an elaboration of synaptic boutons. There is precedent in Drosophila for both types of mechanisms. In fact, in *dnc* mutants, which have increased transmitter release, there is both an elaboration of synaptic boutons and a change in the calcium dependence of transmitter release (Zhong and Wu, 1991; Zhong et al., 1992). These mutants also show a loss of facilitation following high frequency stimulation. We wished to assess whether any of these phenomena were operating at the synapse of glutamate receptor mutants.

We have counted synaptic boutons on the muscle pair (muscles 6 and 7, segment A3) from which the physiological recordings were made. We find a small but significant decrease in bouton number in the mutant (74 ± 4 [$n = 33$] versus 96 ± 4 [$n = 36$]; $p < 0.001$). Since this difference is opposite in sign to the change in transmitter release, the physiological up-regulation in the mutant cannot be explained by structural plasticity leading to an elaboration of boutons. However, we can not rule out an ultrastructural change leading to an increase in the number of release sites.

To assess any change in the calcium dependence of transmitter release in the mutant, we have analyzed quantal content in a range of external calcium concentrations. In all concentrations tested, there is an increase in quantal content in the DGluRIIA mutant compared to wild type that averages over 300% (Figure 6). The slope of the log [Ca^{2+}] versus log [quantal content] is a measure of the calcium dependence of neurotransmitter release and is taken to represent the number of calcium ions required to trigger the fusion of a synaptic vesicle (Dodge and Rahaminoff, 1967). Both mutant and wild-type genotypes have a slope of 4.5, indicating that there is no change in the calcium dependence of release. Therefore, the increase in transmitter release in the mutant is probably not due to a change in the calcium sensor that triggers vesicle fusion.

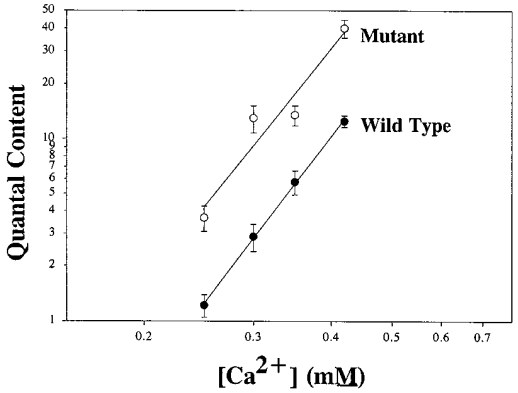

Figure 6. Quantal Content Is Increased Over a Range of Calcium Concentrations

Double-log plot of Ca^{2+} concentration versus quantal content demonstrates that quantal content is increased in the mutant (open circles; *DGluRIIA^{SP16}/Df(2L)cl^{h4}*) compared to wild type (closed circles; *Canton S*) over a range of Ca^{2+} concentrations. The Ca^{2+} dependency is unchanged with a slope of 4.5 in both genotypes. Data are the mean ± SEM from at least nine cells for each genotype at each Ca^{2+} concentration.

Short-term facilitation is another calcium-dependent process that could be affected in a mutant with an increase in basal synaptic transmission. We find no difference in the magnitude of facilitation between wild-type and *DGluRIIA* mutant synapses at either 10 Hz (140% ± 16% [$n = 6$] versus 152% ± 15% [$n = 7$]) or 20 Hz (173% ± 13% [$n = 9$] versus 180% ± 22% [$n = 8$]) stimulation frequencies.

Overexpression of DGluRIIA Leads to an Increase in Quantal Size With No Compensatory Down-Regulation of Quantal Content

Having demonstrated that decreased postsynaptic activity leads to an up-regulation of presynaptic function, we investigated whether increased postsynaptic activity would down-regulate transmitter release. To perform these experiments, we took advantage of the Gal4/UAS system (Brand and Perrimon, 1993) to overexpress DGluRIIA. A transgenic line containing the *DGluRIIA* cDNA cloned downstream of the yeast UAS promoter was crossed to a second line, which strongly expresses the yeast transcription factor Gal4 in all somatic muscles. Since the *UAS–DGluRIIA* insert is on the X chromosome, dosage compensation will lead to a ~2-fold higher level of transgene expression in males than in females.

Intracellular recordings revealed that overexpression of DGluRIIA results in bigger spontaneous events (Figure 7A). The mean mEJP amplitude in control larvae with the Gal4 insert but no *UAS–DGluRIIA* insert (0× transgene expression) was 0.84 ± 0.03 mV. In overexpressing female larvae containing one copy each of *UAS–DGluRIIA* and the Gal4 insert (1× transgene expression), quantal size is increased by 35% (mean mEJP = 1.13 ± 0.06 mV; $p < 0.001$) and in males of the same genotype (2× transgene expression) by 59% (mean mEJP = 1.35 ± 0.06 mV; $p < 0.001$; Figure 7B). Since there was no significant difference in quantal size between the control males and females, the data for these two groups was

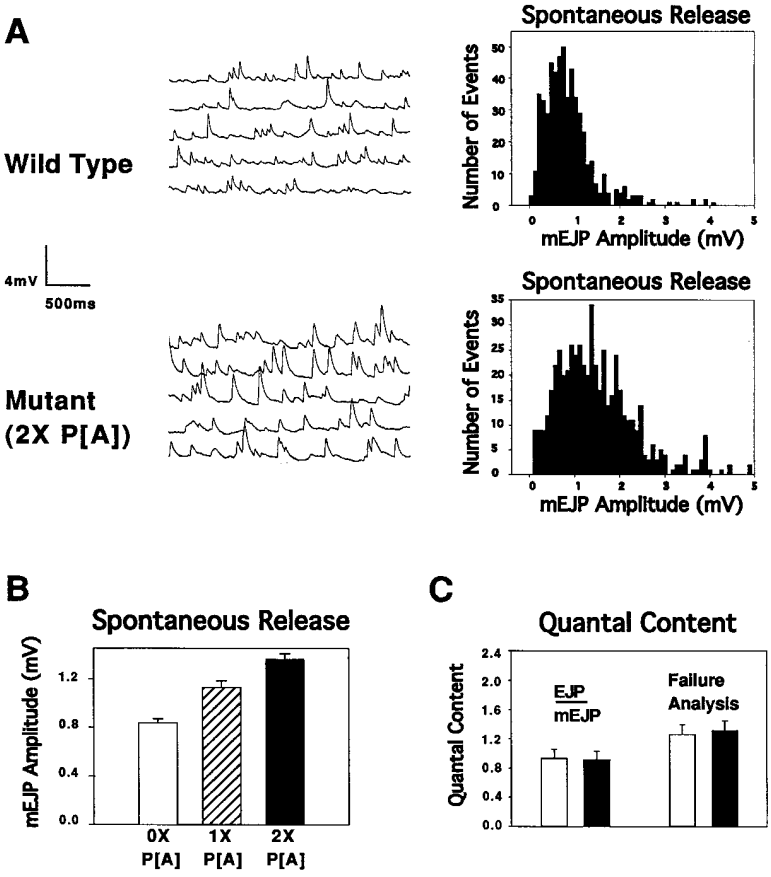

Figure 7. Overexpression of DGluRIIA Leads to an Increase in Quantal Size but No Compensatory Down-Regulation of Quantal Content

(A) Representative traces of spontaneous transmitter release recorded in 0.25 mM calcium from muscle 6, segment A3 of wild-type (*24B Gal4*) and *DGluRIIA* gain-of-function (*24B Gal4* × *UASDGluRIIA*) third instar larvae. Frequency histograms of miniature release event amplitudes (mEJPs) are shown for representative cells of wild-type and *DGluRIIA* gain-of-function larvae that were matched for resting membrane potential.

(B) The mean ± SEM of the mEJP amplitude is shown for 0× overexpressors (*24B Gal4* males and females; open bar; n = 30), 1× overexpressors (*24B Gal4* × *UASDGluRIIA* females; hatched bar; n = 10), and 2× overexpressors (24B Gal4 × *UASDGluRIIA* males; black bar; n = 20). Overexpression of either one or two copies of *DGluRIIA* leads to a significant increase in mEJP amplitude ($p < 0.001$, Student's t test). All three lines had similar resting potentials (*24B Gal4*, −67.5 ± 0.9 mV; *24B Gal4* × *UASDGluRIIA* females, −71.2 ± 1.2 mV; and *24B Gal4* × *UASDGluRIIA* males, −66.0 ± 0.8 mV).

(C) Quantal content estimated by EJP/mEJP amplitudes or failure analysis is not significantly different between 0× overexpressors (*24B Gal4* males; open bar; n = 18) and 2× overexpressors (*24B Gal4* × *UASDGluRIIA* males; closed bar; n = 20). Thus, the increase in quantal size in the 2× overexpressors is not compensated for by a down-regulation of quantal content. (The mean EJP amplitudes are 0.8 ± 0.1 mV for *24B Gal4* males and 1.2 ± 0.2 mV for *24B Gal4* × *UASDGluRIIA* males.)

pooled; however, the increase in quantal size is still highly significant when unpooled data is used. As a second control, data were recorded from male larvae containing a single copy of *UAS–DGluRIIA* but no Gal4. The mean mEJP was 0.90 ± 0.05 mV, a value that is significantly lower than that of the overexpressing females ($p < 0.01$) and males ($p < 0.001$), but is not significantly different than the Gal4 insert control.

Having established that quantal size is increased by overexpression of DGluRIIA, we investigated whether there was a compensatory down-regulation of quantal content in these lines. We calculated quantal content by the method of dividing the mean EJP size by the mean mEJP size (Figure 7C). The mean EJP size was increased (by 52%) while quantal content was virtually identical (0.94 ± 0.12 for control versus 0.92 ± 0.11 for overexpressors). To confirm this result, we performed failure analysis on the two genotypes with the largest difference in quantal size (male larvae with one copy each of Gal4 and *UAS–DGluRIIA* versus male larvae with one copy of Gal4 alone). Quantal content as estimated by failure analysis was extremely similar for the two genotypes (1.26 ± 0.14 for the control Gal4 line versus 1.31 ± 0.14 for overexpressors; Figure 7B). Thus, despite a 59% increase in quantal size, there is no compensatory down-regulation of quantal content, indicating that the retrograde mechanism is insensitive to this level of increase in postsynaptic activity.

Discussion

In this study, we assessed the role of postsynaptic activity in the regulation of synaptic function at the Drosophila neuromuscular junction (NMJ). We identified a novel glutamate receptor, DGluRIIB, that along with the previously described DGluRIIA is expressed specifically by muscle and localizes to synaptic boutons. We generated loss-of-function mutants of *DGluRIIA* that have a decreased quantal size and gain-of-function mutants that overexpress *DGluRIIA* and have an increased quantal size. We find that in the loss-of-function mutants, the decrease in postsynaptic sensitivity is compensated for by an up-regulation of transmitter release from the presynaptic terminal. Hence, the presynaptic neuron is regulated in response to a physiological change in the postsynaptic cell, indicating the existence of a homeostatic mechanism mediated in part by an unknown retrograde signal.

Two Glutamate Receptors at the Neuromuscular Junction

We have demonstrated that at least two glutamate receptors are expressed by Drosophila muscles and are localized to the NMJ. The presence of two receptors may provide the synapse with added flexibility in regulating synaptic strength. The two genes are adjacent in the genome, have similar genomic organization, and are more

closely related to each other than to any other glutamate receptors. Nonetheless, DGluRIIA and DGluRIIB share only 44% amino acid identity. The sequence of DGluRIIA is identical to vertebrate channels in the putative pore region that is critical for Ca^{2+} permeability, while the sequence of DGluRIIB is divergent. Ca^{2+} influx is regulated by RNA editing of this region in vertebrate channels. We observe no editing in either Drosophila gene; however, it is possible that the divergent DGluRIIB plays the role of an edited subunit and that the relative levels of each receptor regulate channel conductance.

Central neurons that receive excitatory and inhibitory inputs must localize different neurotransmitter receptors to appropriate synaptic boutons. We demonstrate that the Drosophila NMJ is also capable of differentially localizing transmitter receptors to particular synapses converging on a single muscle fiber. Both DGluRIIA and DGluRIIB localize to glutamatergic Type I boutons, but neither is detected at the primarily peptidergic Type II boutons (Jia et al., 1993). Furthermore, these receptors localize to hot spots along the synaptic cleft that appear to be opposite presynaptic active zones. This localization pattern is very different from that of other synaptic proteins, such as the PDZ protein Dlg (Budnik et al., 1996) and the cell adhesion molecule FasII (Schuster et al., 1996a), that are present throughout the postsynaptic side of these boutons. Some vertebrate glutamate receptors are thought to be localized to synaptic sites via interaction with PDZ proteins (Dong et al., 1997). The best studied Drosophila PDZ protein, Dlg, is involved in localizing the Shaker potassium channel and FasII to Type I synapses (Tejedor et al., 1997; Zito et al., 1997). However, Dlg is unlikely to be involved in localizing the Drosophila glutamate receptors, since DGluRIIA and DGluRIIB do not colocalize with Dlg, do not contain the C-terminal amino acid sequence required for interaction with Dlg, and still localize in a *dlg* mutant.

Regulation of Quantal Size

We have demonstrated that by genetically manipulating the levels of DGluRIIA, we are able to both decrease and increase quantal size. This suggests that quantal size may normally be in the middle of its dynamic range and that alterations in the function or expression of DGluRIIA is a potential mechanism for regulating synaptic strength.

What is the mechanism by which changes in the amount of DGluRIIA lead to differences in postsynaptic sensitivity to transmitter? The relationship between gene dosage of DGluRIIA and the mEJP amplitude suggests that the density of channels may be an important determinant of quantal size. This implies that receptors are the limiting factor determining mEJP amplitude and is consistent with data from hippocampal synapses that suggest that glutamate receptors are saturated by a single quantum (Tang et al., 1994). Alternatively, DGluRIIA and DGluRIIB may form channels with different properties. Relative levels of DGluRIIA could regulate the conductance of the channel, with higher proportions of DGluRIIA favoring higher conductance channels.

In addition to changing quantal size, deletion of *DGluRIIA* leads to a reduction in the measured frequency of spontaneous mEJPs. Because there was a change in quantal size, we cannot draw conclusions about the actual presynaptic rate of spontaneous vesicle fusions. However, it is likely that the postsynaptic response in *DGluRIIA* mutants has become so small that some events are lost in the noise of the recording. These events have become functionally silent. This may be analogous to vertebrate central synapses in which regulation of homologous postsynaptic receptors may lead to the generation and elimination of silent synapses (Isaac et al., 1995; Liao et al., 1995).

Retrograde Control of Synaptic Strength

We have demonstrated the existence of a retrograde signaling mechanism at the Drosophila NMJ. Decreased activity in the postsynaptic cell leads to a compensatory increase in presynaptic transmitter release. This mechanism may be used during normal development to ensure that the muscle receives adequate amounts of transmitter during its rapid growth from embryonic to larval stages. As the muscle grows and its input resistance drops, a much larger synaptic current is required to depolarize the muscle and allow for efficient contraction. A retrograde signal would ensure a match between postsynaptic requirements for transmitter and presynaptic release characteristics. During normal development, the muscle requires increasing amounts of transmitter; thus, there may be no need for a mechanism to down-regulate quantal content in the face of increased postsynaptic activity. This is consistent with our finding that increased quantal size does not lead to a down-regulation of quantal content. Similar effects on quantal content are observed when quantal size is modulated by PKA (Davis et al., personal communication).

The vertebrate nervous system may use a similar mechanism to match presynaptic release characteristics with the physiological requirements of target cells. At the vertebrate NMJ, evidence from patients with myasthenia gravis and experimental animal models of myasthenia gravis suggest that blockade of postsynaptic acetylcholine receptors, leading to a decrease in quantal size, results in a compensatory increase in quantal content (Cull-Candy et al., 1980; Plomp et al., 1992). Similar results were obtained in *neuregulin* mutant mice, which express decreased levels of acetylcholine receptors (Sandrock et al., 1997). In the central nervous system, this type of mechanism could be used during the development of synapses such as the climbing fiber-to-Purkinje cell synapse, where presynaptic activity must be of sufficient strength to reliably trigger an action potential in the postsynaptic cell.

The identification of the existence of an unknown retrograde signal at the Drosophila NMJ leaves a number of open questions. First, what is being sensed by the muscle that initiates the generation of this signal? The muscle could respond to synaptic depolarization, or it could be sensitive to a second messenger that is regulated by glutamate receptor function, such as calcium influx. Second, what is the presynaptic target of the postsynaptic signal? We observe no sprouting of synaptic boutons or change in the calcium dependence of transmitter release, suggesting that the increase in

transmitter release is not secondary to gross structural plasticity or to a change in the function of the calcium sensor. The increase in presynaptic release may be due to an increase in calcium influx into the presynaptic terminal or to changes in the function of the release machinery. Third, what is the nature of the retrograde signal initiated by activity in the muscle? In Drosophila, unlike in vertebrates, each muscle is not regulated by a sensory neuron-to-motor neuron circuit, so the mechanism is unlikely to be cellular. Precedent exists for diffusible signals such as nitric oxide and arachidonic acid to function as retrograde signals for synaptic plasticity (Larkman and Jack, 1995). Since the pre- and postsynaptic cell are in tight apposition throughout development, the signal could also involve membrane-bound molecules. These questions will be the subject of future genetic and physiological analysis.

Experimental Procedures

Cloning and Molecular Analysis

A clone with homology to *DGluRII* was identified from a cDNA library enriched in trans-membrane proteins (Kopczynski et al., 1996). This clone was amplified by PCR and used as a probe to isolate several cDNA clones from a 9–12 hr λgt11 library using standard methods. Additional clones were isolated from a λzap larval library. Genomic DNA encoding the two receptors was subcloned from P1 phagemids covering the 25F region (gift of C. Schuster). Sequencing was performed on an ALF sequencer (Pharmacia), and analysis was done using Lasergene software. Both strands of a single complete *DGluRIIB* cDNA were sequenced at least twice, partial sequence was obtained from multiple independent *DGluRIIB* clones, and a single strand of the genomic DNA was sequenced.

For the myc-tagged DGluRIIA and DGluRIIB, the signal sequence of the Drosophila cuticle protein CP3 followed by the epitope c-myc (Basler et al., 1991) was inserted into *DGluRIIB* at the NarI site in the N terminus and into *DGluRIIA* at the PvuI site in the N terminus. These constructs were cloned into a transformation vector downstream of the *MHC* promotor (Wassenberg et al., 1987).

Mutations in *DGluRIIA*

A local P-element hopping strategy (Tower et al., 1993) was used to mutate *DGluRIIA*. The starting line (*P[w$^+$11511]* from the Spradling collection) contained a lethal insert in the *n-lamin* gene 15 kb upstream of *DGluRIIA* (Figure 3). The P element was mobilized, and progeny were screened in pools or singly using long-range PCR (XL-PCR kit) on genomic DNA. One of the primers was directed against the end-terminal repeats of the P element, while the other was directed against sequences in *DGluRIIA* or *DGluRIIB*. A second line, *P[w$^+$176]*, was recovered containing a new insert 300 bp upstream of *DGluRIIA*. *P[w$^+$11511]* was excised precisely to generate the line *P[w$^+$60]* and the line *P[w$^+$228]*. The precise excision reverted the lethality of *P[w$^+$11511]* in combination with independent *n-lamin* alleles. Long-range PCR indicated that *P[w$^+$60]* lacks the 8 kb immediately upstream of the remaining insert. The P element was imprecisely excised to produce the mutant line *SP16*, in which a large portion of the extracellular domain of DGluRIIA has been deleted. A second deletion of DGluRIIA (*AD9*) was made by mobilizing the P element in *P[w$^+$228]* to generate a line with a second P element (*P[w$^+$72]*) between *DGluRIIA* and *DGluRIIB*. The two P elements were excised together to remove the entire *DGluRIIA* coding region. More than 5000 lines were analyzed by long-range PCR in this series of hops and excisions.

Genetic Stocks and Crosses for Physiology

Df(2L)cl^{h4} is a deficiency that removes both glutamate receptors, *n-lamin*, and several other lethal genes. *sz15* is a lethal allele that fails to complement *P[w$^+$11511]*; it and the deficiency were used in complementation testing to ensure that *P[w$^+$11511]* had been precisely excised from *n-lamin* (both were the gift of J. Szidonya). *UAS–DGluRIIA* contains the complete *DGluRIIA* cDNA cloned in the pUAST vector (Brand and Perrimon, 1993) inserted on the X chromosome. *24B* is an enhancer trap line expressing Gal4 in all embryonic and larval somatic muscles (Brand and Perrimon 1993). *Δ2–3/TMS,Dr* was the source of transposase used to mobilize P elements. The transgenic rescue line *P[DGluRIIAg]* contains a genomic fragment extending from the EcoRI site 1 kb upstream of *DGluRIIA* to the EcoRI site in *DGluRIIB*.

For the *DGluRIIA* mutant physiology experiments, *(DGluRIIA^{SP16}/Gla,Bc)*, *(DGluRIIA^{AD9}/Gla,Bc)* or *(P[w$^+$228])* flies were crossed to *(Df(2L)clh4/Gla,Bc)* and *Bc$^+$* female larvae were selected for analysis. To rescue the physiological phenotype, *(DGluRIIA^{SP16}/Gla,Bc)* was crossed to *(P[DGluRIIAg]/Y;Df(2L)cl^{h4}/Gla,Bc)*. For the overexpression study, females homozygous for *UAS–DGluRIIA* were crossed to homozygous *24B* males, and male or female larvae were used for analysis as indicated.

Light Microscopy

RNA in situs (Tautz and Pfeifle, 1989), larval dissections, DAB immunochemistry, and myc staining (Johansen et al., 1989; Xu and Rubin, 1995) were performed as previously described. The myc antibody 1–9E10.2 was used at a concentration of 1:10, synaptotagmin antibody (Littleton et al., 1993) was used at a concentration of 1:2000, and flourescent secondary antibodies were used at a concentration of 1:1000.

Immunoelectron Microscopy

Third instar larvae expressing myc-tagged DGluRIIA or DGluRIIB were immobilized, opened dorsally to remove the gut, and prepared for immunoelectron microscopy according to procedures described previously (Lin et al., 1994), with the following modifications. The fixed larvae were incubated sequentially with myc antibody 1–9E10.2 at a concentration of 1:5, with biotinylated goat anti-mouse secondary antibody (1:100) for 1–2 hr, and then with streptavidin-conjugated horseradish peroxidase (HRP; 1:100) for 1–2 hr. Hydrogen peroxide (0.01%) was used instead of glucose oxidase for the reaction between HRP and diaminobenzidine (DAB).

Physiology

Intracellular recordings were made from muscle 6, segment A3 in third instar larvae. The larvae were dissected in physiological saline HL3 (Stewart et al., 1994) containing the indicted Ca^{2+} concentrations. Except where otherwise noted, all recordings were from female larvae. Data were used when the input resistance of the muscle was greater than 5 MΩ and the resting membrane potential was between −60 mV and −80 mV. The larval NMJ was visualized with a compound microscope (Ziess) modified with a fixed-stage and water-immersion lens. Sharp electrodes were filled with 3 M KCl, had a resistance of 15–25 MΩ, and were made of borosilicate glass (outer diameter, 1 mm). Recordings were performed using an Axoclamp 2B. Data were filtered at 1 kHz, digitized, and recorded to disk using a Digidata 1200 analog-to-digital board and PCLAMP6 software. Stimulation of the segmental nerve was achieved by pulling the cut end of the nerve into a suction electrode and passing brief depolarizing pulse (75 ms) with the MASTER-8 stimulus generator and stimulus isolation unit.

To calculate mEJP mean amplitudes, mEJPs were measured by hand using the cursor option in the clampfit software, and amplitudes were averaged. Mean EJP size was calculated by measuring the amplitude of the computer-generated trace average of EJP traces. Quantal content was calculated by dividing the mean EJP by the mean mEJP. Since data were recorded in low calcium saline and EJP amplitudes were small, no correction was made for nonlinear summation. For failure analysis, 400–500 evoked responses were recorded in 0.25 mM Ca^{2+}. For the loss-of-function DGluRIIA experiments, peak amplitudes were measured by hand; when no obvious peaks were identified, measurement of amplitude was made using the cursor positions from the previous trace. For each cell, noise was measured by recording the amplitude difference in a 10 ms window from the prestimulus interval of 250 events. For the DGluRIIA overexpressors, evoked events were measured by setting the cursors to the positions at which maximum amplitude was measured in the trace average. For each cell, noise was measured from

250 traces by setting the cursors close together immediately before the stimulus artifact. Histograms were calculated for EJPs, noise, and mEJPs and compared to determine the proportion of the events that were failures. Quantal content was calculated by the formula quantal content = ln (trials/failures).

Acknowledgments

We thank Christoph Schuster for advice and encouragement throughout these studies; Graeme Davis and Karen Zito for technical assistance, helpful discussions, and critical reading of the manuscript; and Y. Kidokoro for the gift of antisera. Supported by Helen Hay Whitney and Damon Runyon–Walter Winchell Postdoctoral Fellowships to A.D. S.A.P. is a Predoctoral Fellow, R.D.F. is a Senior Research Associate, J.N.N. is a Postdoctoral Fellow, and C.S.G. is an Investigator with the Howard Hughes Medical Institute.

Received September 26, 1997; revised November 5, 1997.

References

Atwood, H.L., Govind, C.K., and Wu, C.-F. (1993). Differential ultrastructure of synaptic terminals on ventral longitudinal abdominal muscles in Drosophila larvae. J. Neurobiol. *24*, 1008–1024.

Bailey, C.H., Bartsch, D., and Kandel, E.R. (1996). Toward a molecular definition of long-term memory storage. Proc. Natl. Acad. Sci. USA *93*, 13445–13452.

Basler, K., Christen, B., and Hafen, E. (1991). Ligand-independent activation of the sevenless receptor kinase changes the fate of cells in the developing Drosophila eye. Cell *64*, 1069–1081.

Betz, H., Schuster, C., Ultsch, A., and Schmitt, B. (1993). Molecular biology of ionotropic glutamate receptors in Drosophila melanogaster. Trends Pharmacol. Sci. *14*, 428–431.

Brand, A.H., and Perrimon, N. (1993). Targeted gene expression as a means of altering cell fates and generating dominant phenotypes. Development *118*, 401–415.

Budnik, V., Zhong, Y., and Wu, C.-F. (1990). Morphological plasticity of motor axons in Drosophila mutants with altered excitability. J. Neurosci. *10*, 3754–3768.

Budnik, V., Koh, Y.-H., Guan, B., Hartmann, B., Hough, C., Woods, D., and Gorczyca, M. (1996). Regulation of synapse structure and function by the Drosophila tumor suppresser gene *dlg*. Neuron *17*, 627–640.

Cline, H.T. (1991). Acivity-dependent plasticity in the visual systems of frogs and fish. Trends Neurosci. *14*, 104–111.

Cull-Candy, S.G., Miledi, R., Trautmann, A., and Uchitel, O.D. (1980). On the release of transmitter at normal, myasthenia gravis and myasthenic syndrome affected human end-plates. J. Physiol. *299*, 621–638.

Currie, D.A., Truman, J.W., and Burden, S.J. (1995). Drosophila glutamate receptor RNA expression in embryonic and larval muscle fibers. Dev. Dyn. *203*, 311–316.

Craig, A.M., Blackstone, C.D., Huganir, R.L., and Banker, G. (1993). The distribution of glutamate receptors in cultured rat hippocampal neurons: postsynaptic clustering of AMPA-selective subunits. Neuron *10*, 1055–1068.

Dan Y., and Poo, M.-M. (1994). Retrograde interactions during formation and elimination of neuromuscular synapses. Curr. Opin. Neurobiol. *4*, 95–100.

Davis, G.W., Schuster, C.M., and Goodman, C.S. (1996). Genetic dissection of structural and functional components of synaptic plasticity. III. CREB is necessary for presynaptic functional plasticity. Neuron *17*, 669–679.

DiAntonio, A., Burgess, R.W., Chin, A.C., Deitcher, D.L., Scheller, R.H., and Schwarz, T.L. (1993). Identification and characterization of Drosophila genes for synaptic vesicle proteins. J. Neurosci. *13*, 4924–4935.

Dodge, F.A., and Rahaminoff, R. (1967). Cooperative action of calcium ions in transmitter release at the neuromuscular junction. J. Physiol. *193*, 419–432.

Dong, H., O'Brien, R.J., Fung, E.T., Lanahan, A.A., Worley, P.F., amd Huganir, R.L. (1997). GRIP: a synaptic PDZ domain-containing protein that interacts with AMPA receptors. Nature *386*, 279–284.

Goodman, C.S., and Shatz, C.J. (1993). Developmental mechanisms that generate precise patterns of neuronal connectivity. Cell *72*/ Neuron *10*, 77–98.

Isaac, J.T.R., Nicoll, R.A., and Malenka, R.C. (1995). Evidence for silent synapses: implications for the expression of LTP. Neuron *15*, 427–434.

Jan, L.Y., and Jan, Y.N. (1976). Properties of the larval neuromuscular junction in Drosophila melanogaster. J. Physiol. *262*, 189–214.

Jia, X.-X., Gorczyca, M., and Budnik, V. (1993). Ultrastructure of neuromuscular junctions in Drosophila: comparison of wild type and mutants with increased excitability. J. Neurobiol. *24*, 1025–1044.

Johansen, J., Halpern, M.E., Johansen, K.M., and Keshishian, H. (1989). Stereotypic morphology of glutamatergic synapses on identified muscle cells of Drosophila larvae. J. Neurosci. *9*, 710–725.

Jonas, P., and Burnashev, N. (1995). Molecular mechanisms controlling calcium entry through AMPA-type glutamate receptor channels. Neuron *15*, 987–990.

Kopczynski, C.C., Davis, G.W., and Goodman, C.S. (1996). A neural tetraspanin, encoded by late bloomer, that facilitates synapse formation. Science *271*, 1867–1870.

Larkman, A.U., and Jack, J.J.B. (1995). Synaptic plasticity: hippocampal LTP. Curr. Opin. Neurobiol. *5*, 324–334.

Liao, D., Hessler, N.A., and Malinow, R. (1995). Activation of postsynaptically silent synapses during pairing-induced LTP in CA1 region of hippocampal slice. Nature *375*, 400–404.

Lin, D.M., Fetter, R.D., Kopczynski, C., Grenningloh, G., and Goodman, C.S. (1994). Genetic analysis of Fasciclin II in Drosophila: defasciculation, refasciculation, and altered fasciculation. Neuron *13*, 1055–1069.

Littleton, J.T., Bellen, H.J., and Perin, M.S. (1993). Expression of synaptotagmin in Drosophila reveals transport and localization of synaptic vesicles to the synapse. Development *118*, 1077–1088.

Nguyen, Q.T., and Lichtman, J.W. (1996). Mechanism of synapse disassembly at the developing neuromuscular junction. Curr. Opin. Neurobiol. *6*, 104–112.

Plomp, J.J., van Kempen, G.T.H., and Molenaar, P.C. (1992). Adaptation of quantal content to decreased postsynaptic sensitivity at single endplates in α-Bungarotoxin-treated rats. J. Physiol. *458*, 487–499.

Rubio, M.E., and Wenthold, R.J. (1997). Glutamate receptors are selectively targeted to postsynaptic sites in neurons. Neuron *18*, 939–950.

Saitoe, M., Tanaka, S., Takata, K., and Kidokoro, Y. (1997). Neural activity affects distribution of glutamate receptors during neuromuscular junction formation in Drosophila embryos. Dev. Biol. *184*, 48–60.

Sandrock, A.W., Dryer, S.E., Rosen, K.M., Gozani, S.N., Kramer, R., Theill, L.E., and Fischbach, G.D. (1997). Maintenance of acetylcholine receptor number by neuregulins at the neuromuscular junction in vivo. Science *276*, 599–603.

Schuster, C.M., Ultsch, A., Schloss, P., Cox, J.A., Schmitt, B., and Betz, H. (1991). Molecular cloning of an invertebrate glutamate receptor subunit expressed in Drosophila muscle. Science *254*, 112–114.

Schuster, C.M., Davis, G.W., Fetter, R.D., and Goodman, C.S. (1996a). Genetic dissection of structural and functional components of synaptic plasticity. I. Fasciclin II controls synaptic stabilization and growth. Neuron *17*, 641–654.

Schuster, C.M., Davis, G.W., Fetter, R.D., and Goodman, C.S. (1996b). Genetic dissection of structural and functional components of synaptic plasticity. II. Fasciclin II controls presynaptic structural plasticity. Neuron *17*, 655–667.

Sheng, M. (1996). PDZs and receptor/channel clustering: rounding up the latest suspects. Neuron *17*, 575-578.

Stewart, B.A., Atwood, H.L., Renger, J.J., Wang, J., and Wu, C.-F. (1994). Improved stability of Drosophila larval neuromuscular preparations in haemolymph-like physiological solutions. J. Comp. Physiol. [A] *175*, 179–191.

Stewart, B.A., Schuster, C.M., Goodman, C.S., and Atwood, H.L. (1996). Homeostasis of synaptic transmission in Drosophila with genetically altered nerve terminal morphology. J. Neurosci. *16*, 3877–3886.

Tang, C.-M., Margulis, M., Shi, Q.-Y., and Fielding, A. (1994). Saturation of postsynaptic glutamate receptors after quantal release of transmitter. Neuron *13*, 1385–1393.

Tautz, D., and Pfeifle, C. (1989). A nonradioactive in situ hybridization method for the localization of specific RNAs in Drosophila embryos reveals translational control of the segmentation gene hunchback. Chromosoma *98*, 81–85.

Tejedor, F.J., Bokhari, A., Rogero, O., Gorczyca, M., Zhang, J., Kim, E., Sheng, M., and Budnik, V. (1997). Essential role for *dlg* in synaptic clustering of Shaker K^+ channels in vivo. J. Neurosci. *17*, 152–159.

Tower, J., Karpen, G.H., Craig, N., and Spradling, A.C. (1993). Preferential transposition of Drosophila P elements to nearby chromosomal sites. Genetics *133*, 347–359.

Wang, J., Renger, J.J., Griffith, L.C., Greenspan, R.J., and Wu, C.-F. (1994). Concomitant alterations of physiological and developmental plasticity in Drosophila CaM kinase II-inhibited synapses. Neuron *13*, 1373–1384.

Wassenberg, D.R., II, Kronert, W.A., O'Donnell, P.T., Bernstein, S.I. (1987). Analysis of the 5′ end of the Drosophila muscle myosin heavy chain gene. Alternatively spliced transcripts initiate at a single site and intron locations are conserved compared to myosin genes of other organisms. J. Biol. Chem. *262*, 10741–10747.

Wo, Z.G., and Oswald, R.E. (1995). Unraveling the modular design of glutamate-gated ion channels. Trends Neurosci. *18*, 161–168.

Xu, T., and Rubin, G.M. (1993). Analysis of genetic mosaics in developing and adult Drosophila tissues. Development *117*, 1223–1237.

Zhong, Y., and Wu, C.-F. (1991). Altered synaptic plasticity in Drosophila memory mutants with a defective cyclic AMP cascade. Science *251*, 198–201.

Zhong, Y., and Shanley, J. (1995). Altered nerve terminal arborization and synaptic transmission in Drosophila mutants of cell adhesion molecule Fasciclin I. J. Neurosci. *15*, 6679–6687.

Zhong, Y., Budnik, V., and Wu, C.-F. (1992). Synaptic plasticity in Drosophila memory and hyperexcitable mutants: role of cAMP cascade. J. Neurosci. *12*, 644–651.

Zito, K., Fetter, R.D., Goodman, C.S., and Isacoff, E.Y. (1997). Synaptic clustering of Fasciclin II and Shaker: essential targeting sequences and role of Dlg. Neuron *19*, 1007–1016.